A Rational Encapsulation Process By Use of an Annular Jet

Lin, S.P. and Chen, J.N.
Department of Mechanical and Aeronautical Engineering
Clarkson University
Potsdam, NY 13699-5725

An annular liquid jet possesses two fluid-fluid interfaces. There exist two independent interfacial modes of natural frequency at the onset of instability. One mode termed para-sinuous mode displaces the two interfaces almost exactly in-phase, and the other displaces the two interfaces almost exactly out of phase to form a varicose mode. The two independent modes interact in a ten flow parameter space. The ten flow parameters are: The Weber numbers associated with the two interfaces, the core to the shell thickness ratio, the ratio of the linear dimension of the reactor to the shell thickness, the viscosity ratio of the core fluid to the shell fluid, the viscosity ratio of the ambient fluid to the shell fluid, the density ratios among three different fluids, Froude number, and the Reynolds number. The sinuous mode is desirable for encapsulation processes, since it tends to maintain a uniform shell thickness and encapsulate the core at its thinnest section. The varicose mode is undesirable, since it tends to vary the shell thickness and pinch off the shell at the location where the core fluid is the thickest, thus leaving the core uncapsulized. Unfortunately the sinuous and varicose modes appear simultaneously in almost the entire region of ten parameter space. The persistent simultaneous appearance of these two modes has made the production of capsules with uniform shell thickness very difficult. It is shown that in certain regions of ten parameter space, the two modes can be separated by use of microgravity. Moreover, the desirable sinuous mode can be resonated by use of appropriate external excitation, while the undesirable varicose mode can be purged. However, this mode selection for favorable encapsulation processes must be performed outside of a region of absolute instability in the parameter space since a continuous encapsulation cannot be achieved in this region.

1. Introduction

The occurrence of multimode instability at the onset is inevitable in many fluid flow systems involving more than one interface. Multimode interfacial instability is encountered in various important scientific and industrial processes. These processes include: coating of films [1-6] production of laminated advanced material [7], transport drag reduction by lining the tube wall with a less viscous fluid [8], encapsulation of more than one pharmaceutical material [9]

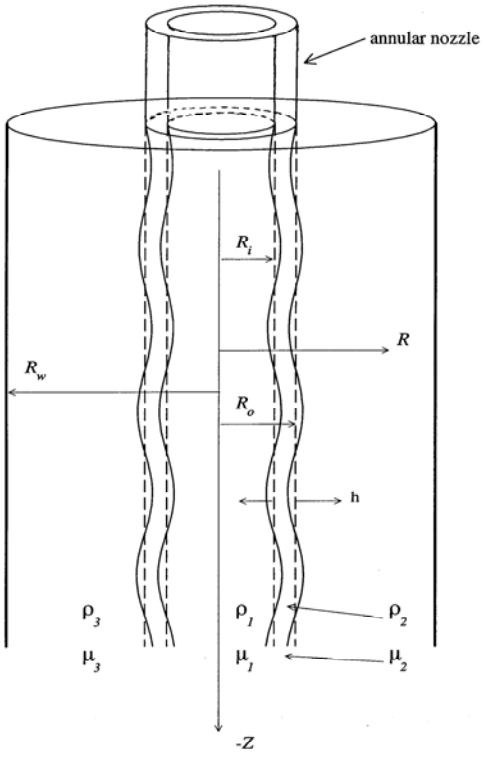

Fig. 1. Annular jet

for direct delivery of a biodegradable microsphere [10], focused dosage application to cancer cells [11] and gene transfer [12], and encapsulation of hydrogen isotopes for inertial confinement fusion [13].

Chen and Lin [14] recently showed how the two independent interfacial modes interact in various regions of a 10-parameter space at the onset of convective instability in an annular liquid jet encapsulating another fluid. One mode is undesireable and the other is useful for perfect encapsulation processes The persistent simultaneous appearance of these modes has made a perfect encapsulation very difficult in the past [15-18]. It is explained here how the desirable mode can be isolated from the other by use of microgravity. It is to demonstrated that the isolated mode can be preferentially amplified to initiate a favorable encapsulation process.

2. Theory

A liquid jet with density ρ_2 and viscosity μ_2 emanates from an annular nozzle which is coaxial with a circular cylinder of radius R_w, as shown in Fig. 1. The axis of the cylinder is aligned with the gravitational acceleration **g**. The fluid inside the annular jet has density ρ_1 and viscosity μ_1. The jet is surrounded by another fluid of density ρ_3 and viscosity μ_3. The governing equations of motion of the fluids, assumed to be incompressible are

$$\partial_t \mathbf{V}_j + \mathbf{V}_j \cdot \nabla \mathbf{V}_j = -\frac{1}{\rho_j} \nabla \cdot \boldsymbol{\sigma}_j + \mathbf{g}, \tag{1}$$

$$\nabla \cdot \mathbf{V}_j = 0 \quad (j = 1,2,3), \tag{2}$$

where j = 1,2 and 3 designate the inner fluid, the shell liquid, and the outer gas, respectively, t is time, **V** is the velocity, ρ is the density and **σ** is the stress tensor. For Newtonian fluids

$$\sigma_j = -P\mathbf{I} + \mu_j[\nabla \mathbf{V}_j) + (\nabla \mathbf{V}_j)^T],$$

where P is the pressure, **I** is the identity matrix and μ is the dynamic viscosity.
The corresponding boundary conditions are the non-slip conditions at the pipe inner wall, i.e.

$$\mathbf{V}_3 = 0 \quad at \quad R = R_w, \tag{3}$$

where R is the radial distance in the cylindrical coordinate (R,θ,Z); the continuity of the velocity at each fluid-fluid interface, i.e.

$$\mathbf{V}_1 = \mathbf{V}_2 \quad \text{at} \quad R = R_i, \tag{4}$$
$$\mathbf{V}_2 = \mathbf{V}_3 \quad \text{at} \quad R = R_0, \tag{5}$$

where R_i and R_0 are, respectively, the inner radius and outer radius of the annulus; the kinematic conditions at the interface, i.e.

$$U_{1,3} = (\partial_t + \mathbf{V}_{1,3} \cdot \nabla)R \quad \text{at} \quad R = R_i \quad \text{or} \quad R_0, \tag{6}$$

where U is the radial component of the velocity, and the subscript 1, followed by 3 after a comma designates either fluid 1 or fluid 3; the dynamics boundary condition at the fluid-fluid interfaces,

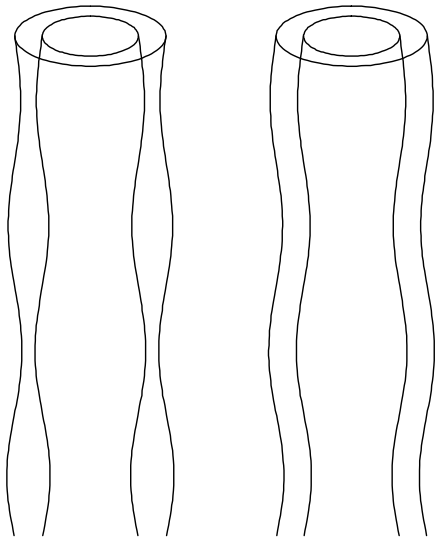

Fig. 2. Schematic of symmetric and antisymmetric disturbances for annular liquid sheet.

$$(\boldsymbol{\sigma}_2 - \boldsymbol{\sigma}_1)\cdot \mathbf{n}_i - \mathbf{n}_i \cdot S_i \nabla \cdot \mathbf{n}_i = 0 \quad \text{at} \quad R = R_i, \tag{7}$$

$$(\boldsymbol{\sigma}_3 - \boldsymbol{\sigma}_2)\cdot \mathbf{n}_o - \mathbf{n}_o \cdot S_o \nabla \cdot \mathbf{n}_o = 0 \quad \text{at} \quad R = R_o, \tag{8}$$

where S_i and S_0 are, respectively, the surface tensions of the inner and the outer interfaces, and $\mathbf{n}_i$ and $\mathbf{n}_0$ are, respectively, the unit normal vectors of the interfaces defined by

$$F_i = R - R_i = 0 \quad and \quad F_0 = R - R_0 = 0. \tag{9}$$

The unit normal vectors at the two interfaces are defined to be positive if they point in a positive radial direction. Thus,

$$(\mathbf{n}_i, \mathbf{n}_0) = (\nabla F/|\nabla F_i|, \nabla F_0/|\nabla F_0|). \tag{10}$$

Based on (1) to (10), Chen and Lin investigate the onset of instability of the annular jet with respect to spatially and temporally growing disturbances in the space of the following parameters:

Weber number of the inner interface $We_i = \rho_2 U^2 h/S_i$,
Weber number of the outer interface $We_o = \rho_2 U^2 h/S_o$,
Reynolds number $Re = \rho_2 U h/\mu_2$,
Froude number $Fr = U^2/gh$,
Viscosity ratios $N_1 = \mu_1/\mu_2$, $N_3 = \mu_3/\mu_2$,
density ratios $Q_1 = \rho_1/\rho_2$, $Q_3 = \rho_3/\rho_2$,
radius ratios $r_1 = R_1/h$, $r_3 = R_3/h$,
where h is the annular shell thickness, and U is the liquid jet velocity at $R = (R_i + R_o)/2$, (cf

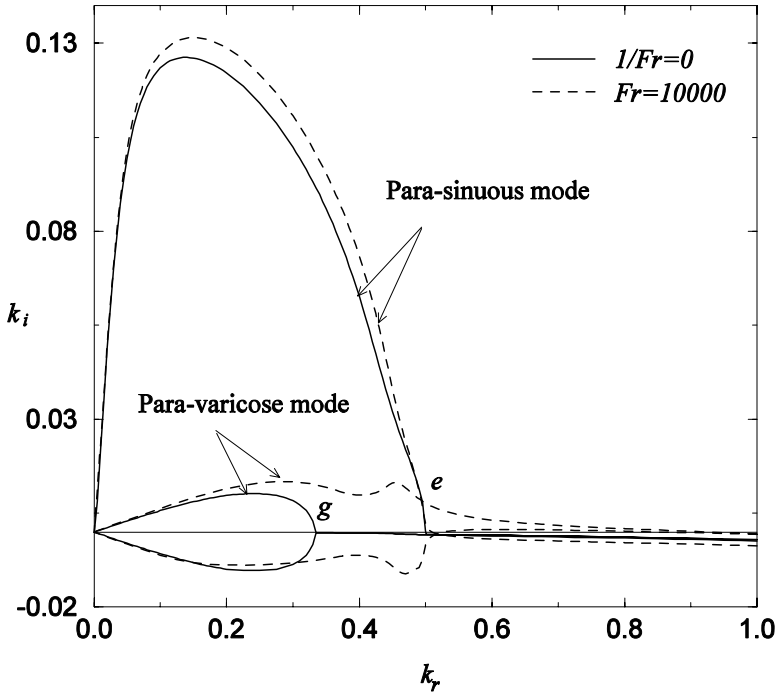

Fig. 3. Isolation of para-sinuous mode by micro-gravity, Re=1000, $We_i = We_0$=20.0, $\overline{N}_1 = \overline{N}_3$=0.018, $Q_1 = Q_3$=0.0013, r_i=2, r_w=13.

Fig. 1). Their results are used here to show how they can be applied to design a rational process of encapsulation.

3. Results

At the onset of convective instability there are two independent modes, para-varicose mode and para-sinuous mode respectively termed symmetric and antisymmetric modes in Fig. 2. In the encapsulation application, the para-varicose mode is undesirable. This is because the liquid annular shell tends to pinch off at a location where the core material is the thickest, leaving the core unencapsulated. On the other hand in the para-sinuous mode the annular shell remains quite uniform and tends to encapsulate the core material at its thinnest location. Therefore the para-sinuous mode must be promoted but the para-varicose mode must be somehow suppressed in order to achieve perfect encapsulation. Unfortunately these two modes emerge simultaneously in general as indicated by two dashed lines for the case of finite gravity in Fig. 3. However, when the gravity is reduced to zero two modes separate as indicated by two solid lines in the same figure. Moreover, in the range of wave number k_r between g and e in Fig. 3, the para-varicose mode has a negative spatial growth rate k_i. Hence the undesirable para-varicose mode is suppressed by microgravity. Therefore if one imparts an external excitation with frequency corresponding to this range of wave number, one may resonate the natural frequency of the sinuous mode to initiate a favorable encapsulation process. In addition, one must also avoid absolute instability, since absolute instability will disallow the continuous process of encapsulation [14,15,20]. Absolute instability does occur in certain parameter space as depicted in Fig. 4. Hence the key to a successful encapsulation process is to operate outside of the absolute instability region, and to suppress the varicose mode in microgravity and to resonate the natural sinuous mode with an appropriate external forcing.

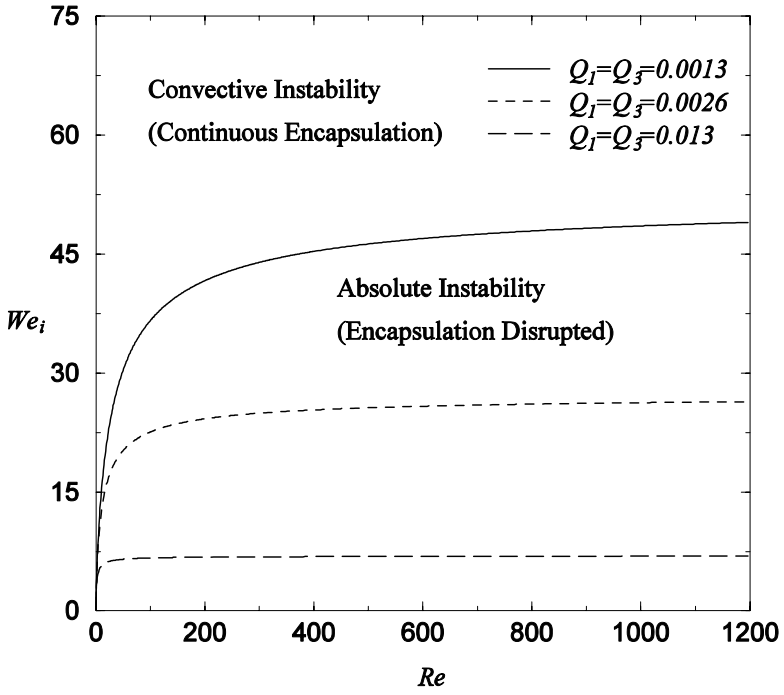

Fig. 4. Critical Weber number for absolute instability, 1/Fr=0.0, $We_i = We_0$, $\overline{N}_1 = \overline{N}_3 = 0.018$, $r_i = 10$, $r_w = 21$.(Forbidden zone for encapsulation)

References

[1] Kao T W 1965 Phys. Fluids **8**, 812-820
[2] Kay T W 1965 Phys. Fluids **8**, 2190-2194
[3] Kay T W 1968 J. Fluid Mech. **33**, 561-572
[4] Loewenherz D S and Lawrence C J 1989 Phys. Fluids A **1**, 1686-1693
[5] Weinstein S J 1990 AIChE J. **36**, 1873-1889
[6] Weinstein S J and Kurz M R 1991 Phys. Fluids A **3**, 2680-2687
[7] Lin S P 1983, J. Fluids Eng. **105**, 119
[8] Chen K and Joseph D D 1991 Phys. Fluids A **3**, 2672-2679
[9] Benita S (Ed.)1996 *Microencapsulation* Marcel Dekker, New York.
[10] Benoit J P Marchois H Rolland H and Velde V p. 35, in ref. 9
[11] Magenheim B and Benita S p. 93 in ref. 9
[12] Furth A 1997 Mol. Biotechnol. **7**, 139
[13] Brady J E and Holum J R 1993 *Chemistry*, p. 1018 John Wiley & Sons, New York
[14] Chen J N and Lin S P 2002 J. Fluid Mech. **450**, 235-258
[15] Lin S P *Breakup of Liquid Sheets and Jets*, 2003 Cambridge Univ. Press
[16] Hertz C H and Hermanrud B 1983 J. Fluid Mech. **131**, 271-287
[17] Kendall J M 1986 Phys. Fluids **29**, 2086-2094
[18] Lee C P and Wang T G 1989 Phys. Fluids A **1**, 967-964
[19] Meyer J and Weihs 1987 J. Fluid Mech. **179**, 531-545
[20] O'Donnell B Chen J N and Lin S P 2001 Phys. Fluids **13**, 2732-2734